



## A general method to determine ionization constants of responsive polymer thin films

Hui Wang<sup>a,b</sup>, Irene H. Lee<sup>a</sup>, Mingdi Yan<sup>a,b,\*</sup>

<sup>a</sup> Department of Chemistry, Portland State University, PO Box 751, Portland, OR 97207-0751, USA

<sup>b</sup> Department of Chemistry, The University of Massachusetts Lowell, One University Ave., Lowell, MA 01854, USA

### ARTICLE INFO

#### Article history:

Received 24 July 2011

Accepted 29 August 2011

Available online 3 September 2011

#### Keywords:

Polymer thin films

Covalent immobilization

Ionization constant

Poly(4-vinylpyridine)

Contact angle titration

Surface plasmon resonance imaging

### ABSTRACT

A general method has been developed to determine the ionization constants of polymer thin films based on the stimuli-responsiveness of the polymer. Robust polymer films were fabricated on silicon wafers and gold slides using perfluorophenyl azide (PFPA) as the coupling agent. The ionization constants were measured by a number of techniques including ellipsometry, dynamic contact angle goniometry, and surface plasmon resonance imaging (SPRI). Using poly(4-vinylpyridine) (P4VP) as the model system, P4VP thin films were fabricated and the ionization constants of the films were measured taking advantage of the pH responsive property of the polymer. The  $pK_a$  determined by ellipsometry,  $\sim 4.0$ , reflects the swelling of the polymer film in response to pH. The  $pK_a$  value calculated from the dynamic contact angle measurements,  $\sim 5.0$ , relies on the change in hydrophilicity/hydrophobicity of the films as the polymer undergoes protonation/deprotonation. The  $pK_a$  value measured by SPRI,  $\sim 4.9$ , monitors *in situ* the change of refractive index of the polymer thin film as it swells upon protonation. This was the first example where SPRI was used to measure the ionization constants of polymers.

© 2011 Elsevier Inc. All rights reserved.

### 1. Introduction

Responsive polymers, whose molecular conformations and polymer chain sizes change in response to the environment conditions such as pH, temperature, light, electric field, solvent, ionic strength, have become an area of high interest and have demonstrated potential in a wide range of applications including sensors, biomedical devices, drug delivery, tissue engineering and microfluidic devices [1–9]. For example, pH-responsive polymers, often containing acidic or basic groups, can swell or collapse upon accepting or releasing protons in response to pH changes in the environment [10–17]. The pH-responsive polymers have been used to form “smart surfaces” in numerous applications such as cell adhesion [18,19], drug delivery [13,15–17], biosensors [14], and microfluidic devices [20].

Because the physical properties of the polymer change in response to external conditions, responsive polymers can be used to determine the related physical parameters of the polymer. For example, Russell et al. determined the elastic property of polymer thin films by measuring the number and length of wrinkles produced by a drop of water placed on a free-floating polymer thin film [21]. In the work of Radmacher and coworkers, gelatin thin films swelled upon treatment with solvents. The apparent Young's

modulus of the film, dependent on the degree of swelling, was subsequently measured by atomic force microscopy [22].

The pH-responsive polymers often contain ionizable groups that associate or dissociate depending on the external pH. The ionization constant is therefore an important parameter in understanding the ionization behavior of pH-responsive polymers as well as in the design of devices based on these polymers [23]. The ionization constant of a pH-responsive polymer thin film may differ from that of the corresponding bulk polymer, since the local environment around the film is different from that in the bulk polymer [24,25].

Various methods have been used to determine the ionization constants of polymer films, including contact angle titration [24,25], electrochemical titration [26], IR spectroscopy [23,27,28], Raman spectroscopy [29], chemical force microscopy [30], neutron reflection [31], and quartz crystal microbalance (QCM) [32]. For example, Mika and Childs determined the  $pK_a$  of P4VP films anchored within the pores of polypropylene microfiltration membranes by potentiometric titrations and changes in membrane thickness [26]. Franck-Lacaze and coworkers measured  $pK_a$  of P4VP films grafted on poly(tetrafluoroethylene-co-hexafluoropropylene) (ARA<sup>TM</sup>) and poly(ethylene-co-tetrafluoroethylene) (AW<sup>TM</sup>) membranes by confocal Raman spectroscopy [29]. Generally, these methods can be divided into two types: sensitive only to the uppermost layer of the polymer film, e.g., contact angle goniometry and chemical force microscopy, and sensitive to the bulk polymer film, e.g., IR spectroscopy and QCM.

\* Corresponding author at: Department of Chemistry, Portland State University, PO Box 751, Portland, OR 97207-0751, USA. Fax: +1 978 934 3013.

E-mail address: mingdi\_yan@uml.edu (M. Yan).



## 2.4. Ellipsometry

Phosphate buffers of varying pH were prepared by mixing  $\text{NaH}_2\text{PO}_4 \cdot \text{H}_2\text{O}$  and  $\text{Na}_2\text{HPO}_4 \cdot 7\text{H}_2\text{O}$  in the appropriate proportions and the pH measured using a pH meter. P4VP films were soaked in each phosphate buffer solution for 10 min, rinsed quickly with water and dried with nitrogen. Film thickness measurements were performed at room temperature ( $\sim 20^\circ\text{C}$ ) on an ellipsometer (Model L116A, Gaertner Scientific Co.) with a He/Ne laser (632.8 nm, 2 mW, Melles Griot) at the incident angle of  $70^\circ$  in the manual mode. The real and imaginary parts of the refractive index of the freshly cleaned gold films were measured to be 0.2275 ( $N_s$ ) and  $-3.4275$  ( $K_s$ ), respectively. The refractive indices ( $N_f$ ) of 1.60 for P4VP [40] and 1.50 for PFPA-disulfide were used in calculating the film thickness. For each sample, three different spots on each sample were chosen and the thicknesses were measured and averaged.

## 2.5. Contact angle measurements

Contact angles were measured on a goniometer (model 250, Ramé–Hart Instrument Co., Netcong, NJ). The advancing contact angle ( $\theta_A$ ) was determined by placing a drop of corresponding buffer from a syringe dispenser attached to the instrument, advancing the periphery of the drop by adding corresponding buffer at the rate of  $0.05 \mu\text{L/s}$  at a time interval of 1.0 s, and recording the contact angle as well as the diameter of the droplet. The receding contact angle ( $\theta_R$ ) was measured by withdrawing buffer from the drop at the same rate and time interval, and recording the contact angle and the diameter of the droplet. The needle was kept inside the buffer droplet throughout the measurements. Data were recorded and analyzed using the DROPimage Advanced v2.2 software provided by Ramé–Hart.

## 2.6. Fabrication of polymer arrays on SPR sensor chips

SPR sensor chips were prepared as follows. High refractive index N-SF10 glass slides ( $18 \text{ mm} \times 18 \text{ mm}$ , SCHOTT Glass Technology, Inc., PA) were cleaned in the piranha solution at room temperature for 60 min and washed thoroughly in boiling water three times for 60 min each. The slides were then dried with nitrogen and coated with a 2 nm thick Ti followed by a 45 nm gold film in an electron beam evaporator (SEC-600, CHA Industries, Fremont, CA) at the Microfabrication Lab, Washington Technology Center (University of Washington).

The SPR chips were cleaned and treated with PFPA-disulfide using the same procedures as those for the regular gold slides described above. P4VP arrays were generated by manually spotting solutions of P4VP in 2-propanol (1 mg/mL) onto the SPR chip using a pipettor tip. The printed SPR chip was dried under vacuum for 20 min. The chip was then irradiated with the medium-pressure Hg lamp, washed thoroughly in 2-propanol for 12 h followed by Milli-Q water for three times at 1 h each, and finally dried under nitrogen.

## 2.7. SPR imaging

SPRi experiments were conducted at room temperature using a SPRiMager<sup>®</sup> II system (GWC Technologies, Inc.). The incident angle was optimized and was kept constant in all experiments. The polymer array chip was primed in pH 7.4 PBS buffer (0.1 M) until a stable baseline was reached. PBS buffers (0.1 M) of various pH were then injected and SPR responses recorded. The flow rate was kept at  $100 \mu\text{L/min}$ . Data acquisition was carried out by selecting the area within printed spots on a microarray image, i.e., region of interest (ROI). An average of 30 images/frames was utilized and SPR signals converted to normalized percentage in reflectivity

( $\% \Delta R$ ) following the protocol provided by GWC. All SPR images were collected and analyzed using the Digital Optics V++ image Version 4 software package provided by the manufacturer.

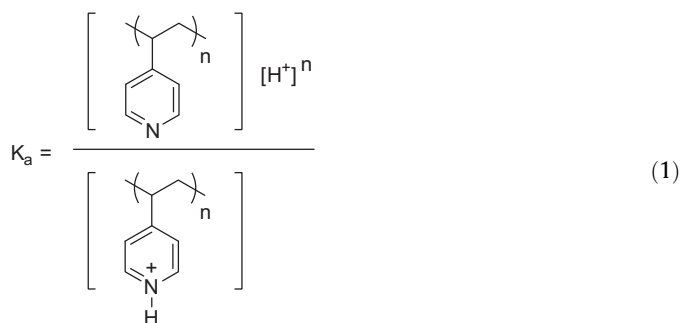
## 3. Results and discussion

### 3.1. Fabrication of P4VP thin films

P4VP thin films were fabricated following a general procedure developed in our laboratory [34,35,37,41]. Briefly, gold slides or wafers were treated with PFPA-disulfide or PFPA-silane to introduce PFPA on the surface (Scheme 1). P4VP was then spin-coated or printed on the PFPA-functionalized surface followed by UV irradiation. The deep UV light emitted from the medium-pressure Hg lamp generates free radicals in P4VP which combine to give cross-linked products [32]. At the same time, UV irradiation converts PFPA to singlet perfluorophenyl nitrene, which undergoes CH insertion reaction with P4VP to covalently attach P4VP to the substrate [37,42–44]. The samples were then soaked in chloroform to remove un-attached polymers, and were dried to give P4VP thin films or arrays (Scheme 1).

### 3.2. Determination of $pK_a$ by ellipsometry

P4VP is a basic polymer that swells upon protonation. The swelling is attributed to the electrostatic repulsion between adjacent charges on the polymer and/or the osmotic pressure effect, where water enters the polymer to equalize the charge density difference between the polymer and the solution [45]. Therefore, by measuring the thickness of the polymer film as a function of pH, the ionization constant can be derived by applying the Hendersen–Hasselbalch equation (Eq. (1)) as the pH when  $[\text{P4VP}] = [\text{P4VPH}^+]$ , i.e., when 50% of the polymer is protonated.



To ensure that the P4VP films adhere well to the substrate, the gold slides were functionalized with PFPA-disulfide before spin-coating P4VP. UV irradiation crosslinked the polymer and at the same time covalently attached the films onto the gold slides via the surface PFPA. The film was then soaked in a pH 7.8 phosphate buffer for 5 min, rinsed quickly with water to remove residual salts, and the film thickness was measured by ellipsometry. This process was repeated using phosphate buffers of different pH, and the film thicknesses were measured after each treatment. Results show that the film thickness increased as the pH of the buffer decreased (Fig. 1a). The P4VP film was expected to protonate at lower pH, therefore the crosslinked polymer film would swell and the film thickness would increase. The data were then fit to a logistic function, and the  $pK_a$  was determined as the pH where the P4VP film thickness was 50% of the maximum when the film was fully protonated and swollen (Eq. (1)). For the data shown in Fig. 1a, curve fitting gave a  $pK_a$  of ca. 4.0 for the P4VP films. This result was similar to the reported  $pK_a$  value of a bulk P4VP polymer (4.0) [46].

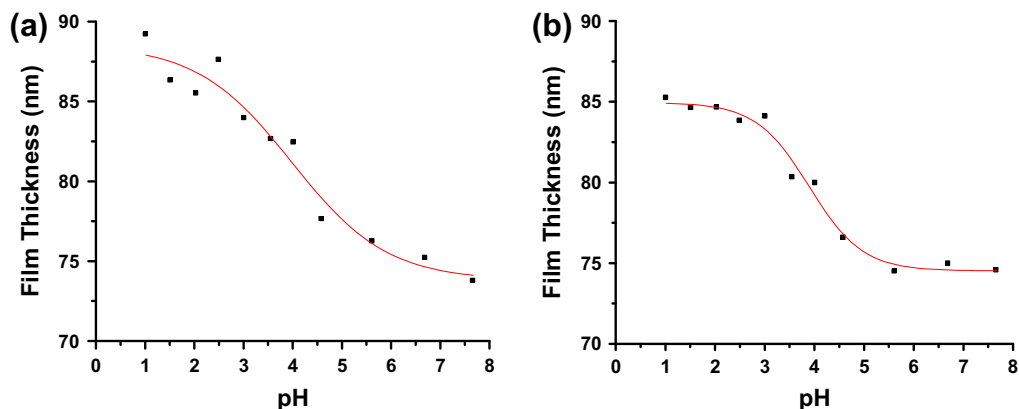


**Fig. 1.** Film thickness of P4VP 160,000 immobilized on gold slides after treating with PBS buffers of varying pH from: (a) high to low and (b) low to high. The experimental data (solid squares) were fitted with the logistic function (lines).

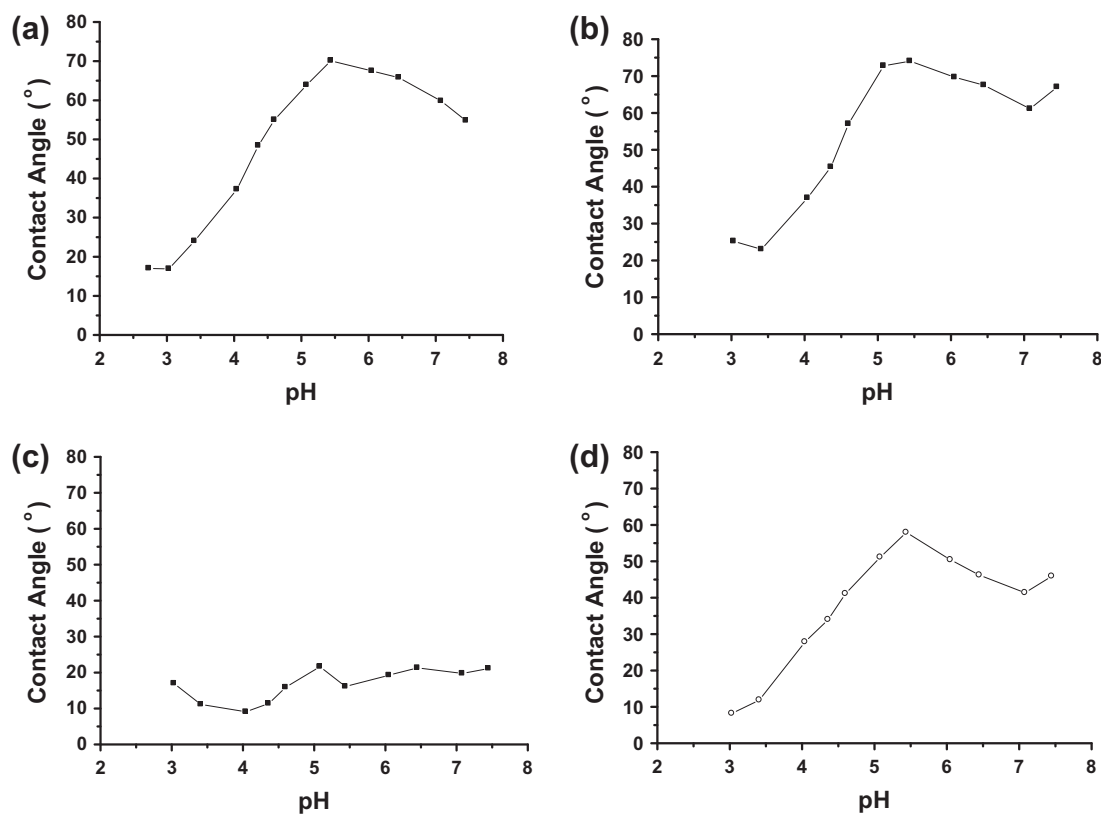


**Fig. 2.** Contact angle titration curves: (a) static, (b) advancing and (c) receding contact angles, and (d) contact angle hysteresis. The experimental data points were connected with lines to aid visualization.

A second set of experiments was carried out where the cross-linked P4VP film was first treated in pH 1.0 buffer, and then with buffers of increasing pH and the film thicknesses were measured. In this case, the cycle began when the film was fully swollen at pH 1.0 and was at its greatest film thickness. As the pH of the buffer increased, the film became thinner (Fig. 1b). Again, an S-shaped curve was obtained when fitting the data with the logistic function (Fig. 1b). The  $pK_a$  value, determined by curve fitting, ca.  $\sim 4.0$ , matches the value obtained from Fig. 1a where the cycle began at pH 7.6 when the film was in the non-swollen state. These results not only demonstrate that the method is reliable, but also confirm that the film swelling is reversible.

### 3.3. Determination of $pK_a$ by contact angle goniometry

The P4VP films prepared by spin-coating from the chloroform solution had a static water contact angle of  $67^\circ \pm 1.9$ . When P4VP is protonated, the film becomes more hydrophilic and the contact angle is expected to decrease. Therefore, by treating the P4VP film with varying pH and measuring the contact angle of the resulting film, the  $pK_a$  value can be derived from the contact angle – pH titration curve. In the experiments, P4VP thin films were immersed in 0.1 M phosphate buffers of varying pH for 10 min each, and dried. The static,  $\theta_A$  and  $\theta_R$  values were then measured using the corresponding buffer solutions, and results were plotted against pH of the buffer (Fig. 2a–c). The contact angle hysteresis, defined as

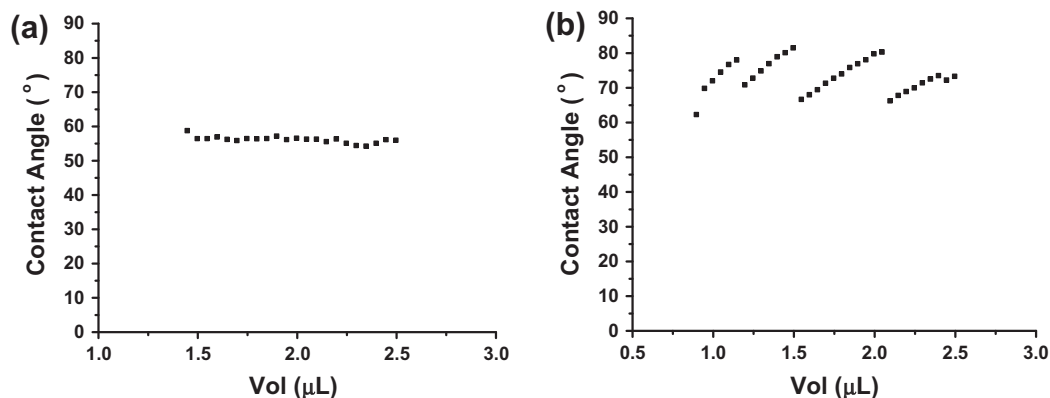


Fig. 3. Advancing contact angle graphs of P4VP films using buffer solution of pH: (a) 4.04 and (b) 5.04.

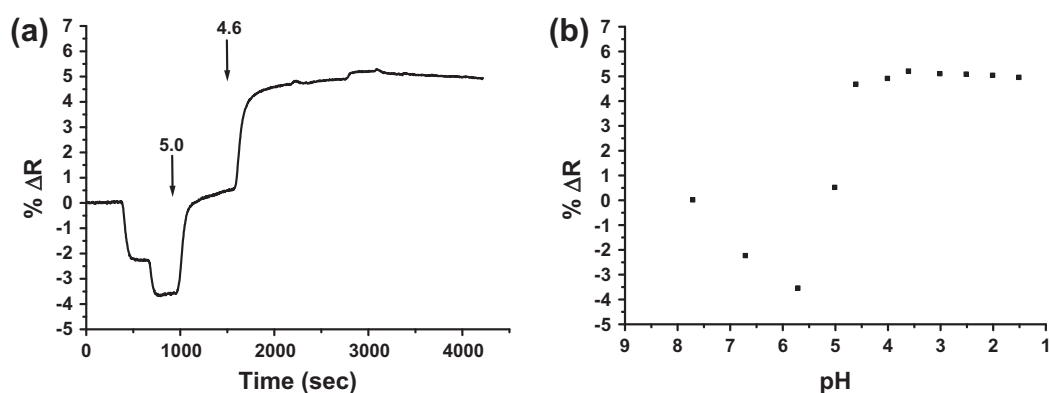


Fig. 4. (a) SPR sensorgram monitoring the percent change in reflectivity as a function of pH. The measurements started in the pH 7.7 PBS buffer (0.1 M), and buffers of pH 6.7, 5.7, 5.0, 4.6, 4.0, 3.6, 3.0, 2.5, 2.0, 1.5 and 1.0 were injected at 5, 10, 15, 25, 35, 45, 50, 55, 60, 65 and 70 min, respectively. Sensorgrams were recorded simultaneously for all spots (see Supporting Information for the array layout and the SPRi image), however, only one response curve was shown for clarity. (b) SPR responses as a function of pH.

$\theta_A - \theta_R$ , was computed from each measurement and the results were plotted against pH (Fig. 2d). Surprisingly, none of the contact angle titration curves showed the anticipated S shape. Instead, both static and advancing contact angles reached their highest values between pH 5.0 and 5.5 (Fig. 2a and b). The receding contact angle also peaked at around pH 5.0 (Fig. 2c), although the value did not change as drastically as the values of the static or the advancing contact angles.

In addition, the hysteresis also reached the highest value between pH 5.0 and 5.5 (Fig. 2d). Generally, the contact angle hysteresis reflects the extent of interactions between the liquid droplet and the surface, and is related to the surface roughness and chemical heterogeneity [47]. A higher hysteresis suggests a surface that is more heterogeneous or rougher. At  $\text{pH} = \text{p}K_a$ , 50% of the pyridyl groups are protonated leaving the other 50% in the un-protonated neutral state. At this point, the P4VP film would be the most heterogeneous chemically. Evidences of this chemical heterogeneity can also be found during the courses of dynamic contact angle measurements. Fig. 3a shows a typical graph of the advancing contact angle measurement where the contact angle remained mostly unchanged throughout the course of the titration [48]. At pH 5.04, however, multiple breaking points were observed during the titration (Fig. 3b), likely due to the heterogeneity of the film.

### 3.4. Determination of $\text{p}K_a$ by SPRi

The pH responsive behavior of the P4VP thin films was further studied using SPRi. SPR is a label-free and real-time sensing technique. In addition, SPRi allows the simultaneous detection of

multiple interactions on an array [49–55] and therefore, different polymers can be spotted and the  $\text{p}K_a$  values measured simultaneously. The samples were prepared by first treating the SPR sensor chips with PFPA-disulfide. P4VP was then spotted on the chip and was subsequently immobilized by UV irradiation. The SPR sensorgrams were obtained by injecting phosphate buffers of varying pH into the flow cell containing the sample, and responses were recorded in real time. The SPR signal, presented as  $\% \Delta R$ , decreased from pH 7.7 to 5.7 (Fig. 4a). The SPR response increased drastically when the pH 5.0 buffer was introduced. The signal continued to increase at pH 4.6, after which, remained relatively constant at pH below 4.0 (Fig. 4a).

The SPR responses, i.e.,  $\% \Delta R$ , were then plotted against pH, and results are shown in Fig. 4b. Ideally, an S curve similar to those in Fig. 1 was to be expected. However, as the pH changed from 7.7 to 6.6 and 5.7, instead of remaining constant, the signal decreased (Fig. 4b). SPR is related to the refractive index of the dielectric layer on the Au surface, and the signal is proportional to the change in the refractive index and surface concentration (mass/area) of the dielectric layer [56]. The drastic increase in the SPR response from pH 5.7 to 4.6 can be attributed to the swelling of the P4VP film where the film thickness increased significantly. The decrease in the SPR signal from 7.8 to 5.7 is puzzling, however. The protonation-induced swelling is minimal in this pH range. A decrease in the SPR response could be caused by a decrease in the refractive index and/or the surface concentration of the P4VP layer, the nature of which is currently under investigation. Assuming minimal swelling in the pH range of 7.8–5.7, the data were fitted to an S curve ( $R^2 = 0.94$ ), from which the  $\text{p}K_a$  value was determined to be  $\sim 4.9$ .

#### 4. Conclusions

In summary, the pH responsive property of P4VP was successfully utilized to measure the ionization constants of P4VP thin films. The films were fabricated by UV irradiation which simultaneously crosslinks the polymer and covalently immobilizes the film. The process is general and simple, and the resulting films were robust and could withstand the experimental conditions including *in situ* measurements at low pH. The  $pK_a$  values were measured by ellipsometry, dynamic contact angle, and SPRi. Ellipsometry monitors the swelling of the polymer films in response to pH and measures the film thickness in the dry state. The contact angle reflects the hydrophilicity/hydrophobicity of the surface layer as the polymer films becomes protonated/deprotonated. Instead of the typical S curve observed in the ellipsometry measurements, the contact angles and hysteresis took the largest value at  $pK_a$ , reflecting the highest chemically heterogeneity of the films at  $pH = pK_a$ . SPR, being a real time sensing technique, reflects the change in refractive index of the polymer film. By monitoring the SPR signals in response to pH *in situ*, the  $pK_a$  value of the P4VP film was successfully determined. This represents the first example where the SPRi technique has been employed to measure the ionization constants of polymer thin films. The method developed is general and can be readily applied to other responsive polymers.

#### Acknowledgment

This work was supported by the National Institutes of General Medical Science (NIGMS) under NIH Award Numbers R01GM080295 and 2R15GM066279.

#### Appendix A. Supplementary data

Supplementary data associated with this article can be found, in the online version, at [doi:10.1016/j.jcis.2011.08.081](https://doi.org/10.1016/j.jcis.2011.08.081).

#### References

- [1] S. Minko, *Responsive Polymer Materials: Design and Applications*, Wiley-Blackwell, 2006.
- [2] Y. Osada, J.P. Gong, *Prog. Polym. Sci.* 18 (1993) 187.
- [3] I. Luzinov, S. Minko, V.V. Tsukruk, *Prog. Polym. Sci.* 29 (2004) 635.
- [4] S.A. Sukhishvili, *Curr. Opin. Colloid Interface Sci.* 10 (2005) 37.
- [5] S. Minko, *Polym. Rev.* 46 (2006) 397.
- [6] S.K. Ahn, R.M. Kasi, S.C. Kim, N. Sharma, Y.X. Zhou, *Soft Matter* 4 (2008) 1151.
- [7] M.A.C. Stuart, W.T.S. Huck, J. Genzer, M. Muller, C. Ober, M. Stamm, G.B. Sukhorukov, I. Szleifer, V.V. Tsukruk, M. Urban, F. Winnik, S. Zauscher, I. Luzinov, S. Minko, *Nat. Mater.* 9 (2010) 101.
- [8] J.L. Zhang, Y.C. Han, *Chem. Soc. Rev.* 39 (2010) 676.
- [9] T. Chen, R. Ferris, J.M. Zhang, R. Ducker, S. Zauscher, *Prog. Polym. Sci.* 35 (2010) 94.
- [10] R. Langer, N.A. Peppas, *AIChE J.* 49 (2003) 2990.
- [11] R.L. Thompson, S.J. Hardman, L.R. Hutchings, A. Narrainen, R.M. Dalglish, *Langmuir* 25 (2009) 3184.
- [12] A.K. Bajpai, J. Bajpai, R. Saini, R. Gupta, *Polym. Rev.* 51 (2011) 53.
- [13] S. Dai, P. Ravi, K.C. Tam, *Soft. Matter* 4 (2008) 435.
- [14] A. Richter, G. Paschew, S. Klatt, J. Lienig, K.F. Arndt, H. Adler, *Sensors* 8 (2008) 561.
- [15] D. Schmaljohann, *Adv. Drug Delivery Rev.* 58 (2006) 1655.
- [16] P. Gupta, K. Vermani, S. Garg, *Drug Discovery Today* 7 (2002) 569.
- [17] Y. Qiu, K. Park, *Adv. Drug Delivery Rev.* 53 (2001) 321.
- [18] J.H. Lee, H.W. Jung, I.K. Kang, H.B. Lee, *Biomaterials* 15 (1994) 705.
- [19] J.M. Goddarda, J.H. Hotchkiss, *Prog. Polym. Sci.* 32 (2007) 698.
- [20] D.J. Beebe, J. Moore, J.M. Bauer, Q. Yu, R.H. Liu, C. Devadoss, B.H. Jo, *Nature* 404 (2000) 588.
- [21] J. Huang, M. Juszkiewicz, W.H.d. Jeu, E. Cerda, T. Emrick, N. Menon, T.P. Russell, *Science* 317 (2007) 650.
- [22] J. Domke, M. Radmacher, *Langmuir* 14 (1998) 3320.
- [23] R. Dong, M. Lindau, C.K. Ober, *Langmuir* 25 (2009) 4774.
- [24] S.R. Holmesfarley, R.H. Reamey, T.J. McCarthy, J. Deutch, G.M. Whitesides, *Langmuir* 1 (1985) 725.
- [25] C.D. Bain, G.M. Whitesides, *Langmuir* 5 (1989) 1370.
- [26] A.M. Miika, R.F. Childs, *J. Membr. Sci.* 152 (1999) 129.
- [27] O. Gershevit, C.N. Suenik, *J. Am. Chem. Soc.* 126 (2004) 482.
- [28] J. Choi, M.F. Rubner, *Macromolecules* 38 (2005) 116.
- [29] L. Franck-Lacaze, P. Sista, P. Huguet, *J. Membr. Sci.* 326 (2009) 650.
- [30] D.V. Vezenov, A. Noy, L.F. Rozsnyai, C.M. Lieber, *J. Am. Chem. Soc.* 119 (1997) 2006.
- [31] S.W. An, R.K. Thomas, *Langmuir* 13 (1997) 6881.
- [32] B. Harnish, J.T. Robinson, Z.C. Pei, O. Ramstrom, M. Yan, *Chem. Mater.* 17 (2005) 4092.
- [33] M.A. Bartlett, M. Yan, *Adv. Mater.* 13 (2001) 1449.
- [34] L. Liu, M. Yan, *Angew. Chem., Int. Ed.* 45 (2006) 6207.
- [35] L. Liu, M.H. Engelhard, M. Yan, *J. Am. Chem. Soc.* 128 (2006) 14067.
- [36] M. Yan, J. Ren, *Chem. Mater.* 16 (2004) 1627.
- [37] M. Yan, *Chem.-Eur. J.* 13 (2007) 4138.
- [38] H. Wang, J. Ren, A. Hlaing, M. Yan, *J. Colloid Interface Sci.* 354 (2011) 160.
- [39] X. Wang, O. Ramstrom, M. Yan, *J. Mater. Chem.* 19 (2009) 8944.
- [40] L.C. Cesteros, J.R. Isasi, I. Katime, *Macromolecules* 27 (1994) 7887.
- [41] M. Yan, B. Harnish, *Adv. Mater.* 15 (2003) 244.
- [42] N. Soundararajan, M.S. Platz, *J. Org. Chem.* 55 (1990) 2034.
- [43] J.F.W. Keana, S.X. Cai, *J. Org. Chem.* 55 (1990) 3640.
- [44] R. Poe, K. Schnapp, M.J.T. Young, J. Grayzar, M.S. Platz, *J. Am. Chem. Soc.* 114 (1992) 5054.
- [45] A. La Rosa, M. Yan, in: A.A. Tseng (Ed.), *Tip-Based Nanofabrication: Fundamentals and Applications*, Springer, New York, 2011, p. 299.
- [46] M. Satoh, E. Yoda, T. Hayashi, J. Komiyama, *Macromolecules* 22 (1989) 1808.
- [47] R.E.J. Johnson, R.H. Dettre, *J. Phys. Chem.* 68 (1964) 1744.
- [48] D.Y. Kwok, T. Gietzelt, K. Grundke, H.J. Jacobasch, A.W. Neumann, *Langmuir* 13 (1997) 2880.
- [49] E. Yeatman, E.A. Ash, *Electron. Lett.* 23 (1987) 1091.
- [50] J. Homola, S.S. Yee, G. Gauglitz, *Sensor Actuators, B* 54 (1999) 3.
- [51] J.M. Brockman, B.P. Nelson, R.M. Corn, *Annu. Rev. Phys. Chem.* 51 (2000) 41.
- [52] M. Bally, M. Halter, J. Voros, H.M. Grandin, *Surf. Interface Anal.* 38 (2006) 1442.
- [53] C. Boozer, G. Kim, S.X. Cong, H.W. Guan, T. Londergan, *Curr. Opin. Biotechnol.* 17 (2006) 400.
- [54] S. Ray, G. Mehta, S. Srivastava, *Proteomics* 10 (2010) 731.
- [55] S. Scarano, M. Mascini, A.P.F. Turner, M. Minunni, *Biosens. Bioelectron.* 25 (2010) 957.
- [56] J. Homola, *Chem. Rev.* 108 (2008) 462.